Electronic Supplementary Material (ESI) for EES Catalysis.


# Supporting Information

## Multichannel Nitrogen-doped Carbon Fibers confined $Fe_3C$ Nanoparticles for Efficient Electroreduction of Nitrate

Fangzhou Zhang,[a] Zhangsheng Shi,[c] Junliang Chen,[a] Hongxia Luo,[a] Jun Chen,*[b] and Jianping Yang*[a]

[a]State Key Laboratory for Modification of Chemical Fibers and Polymer Materials, College of Materials Science and Engineering, Donghua University, Shanghai 201620, P. R. China
[b]ARC Centre of Excellence for Electromaterials Science, Intelligent Polymer Research Institute (IPRI), Australian Institute of Innovative Materials (AIIM), University of Wollongong, Wollongong, NSW 2522, Australia
[c]Department of Chemistry, City University of Hong Kong, Hong Kong SAR, China

E-mail: junc@uow.edu.au; jianpingyang@dhu.edu.cn

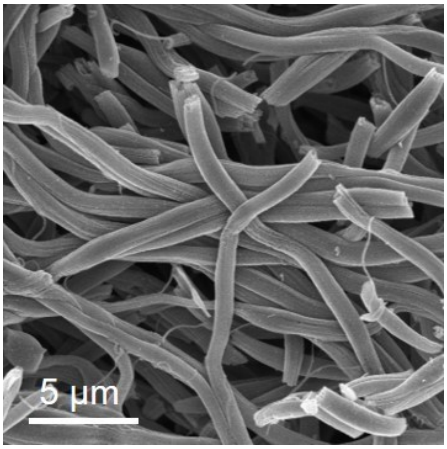


Fig. S1. SEM image of $Fe_3C$/MNCFs-800.

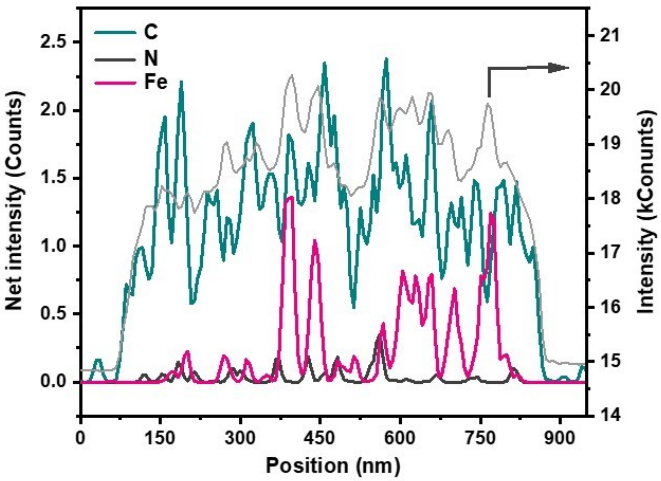


Fig. S2. Line scanning of $Fe_3C$/MNCFs-800.

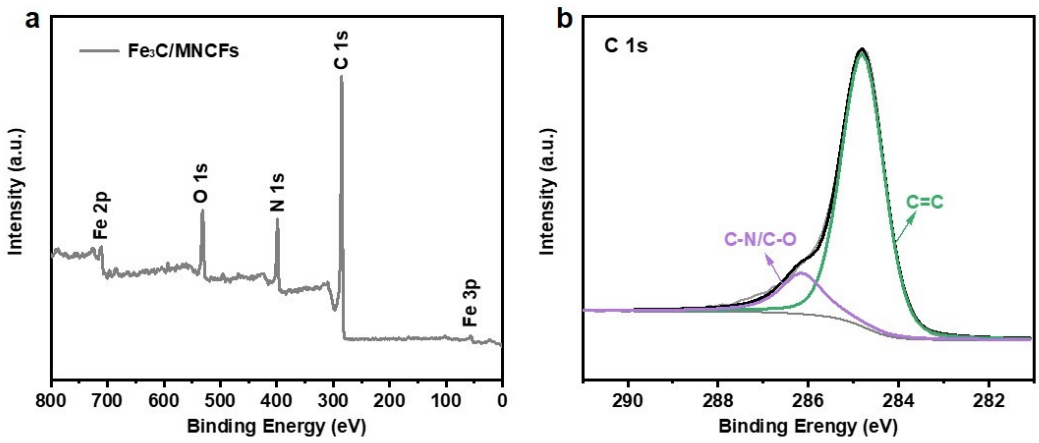


Fig. S3. a) XPS survey spectrum and b) high-resolution C 1s spectrum of $Fe_3C$/MNCFs-800.

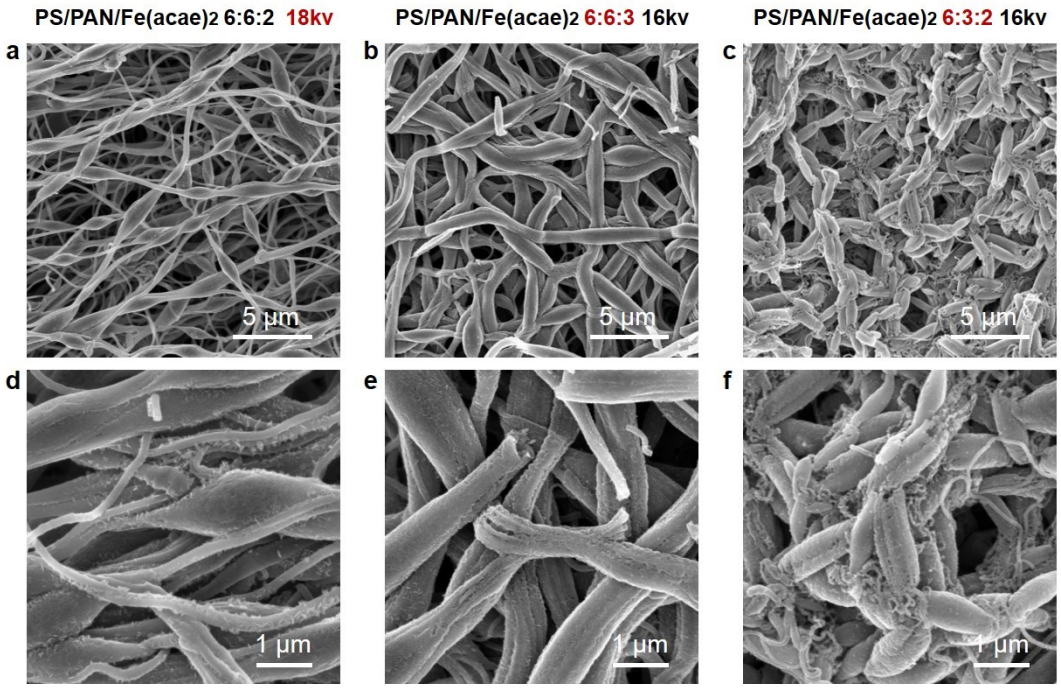


Fig. S4. SEM images of $Fe_3C$/MNCFs-800. a, d) The voltage is 18 kv. b, e) The mass ratio of PS/PAN/Fe(acae)$_3$ is 6:6:3. c, f) The mass ratio of PS/PAN/Fe(acae)$_3$ is 6:3:2.

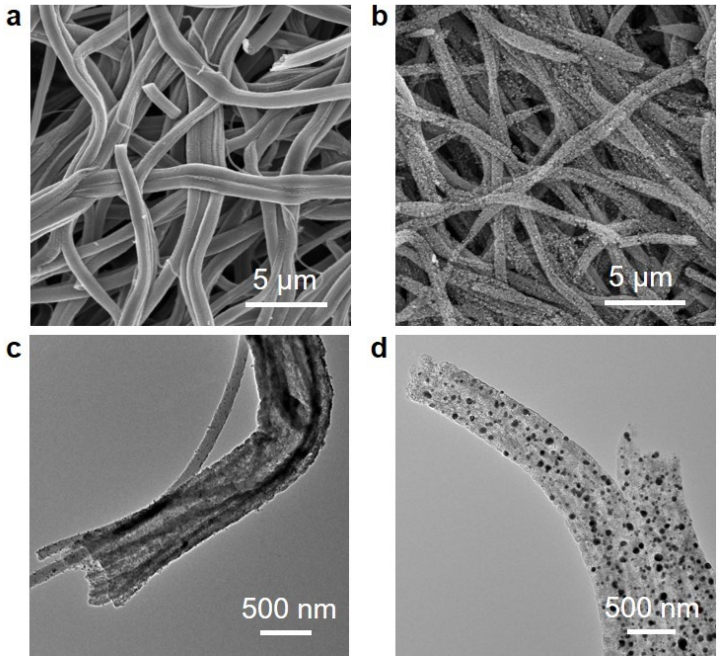


Fig. S5. a) SEM and c) TEM images of $Fe_3C$/MNCFs-700. b) SEM and d) TEM images of $Fe_3C$/MNCFs-900.

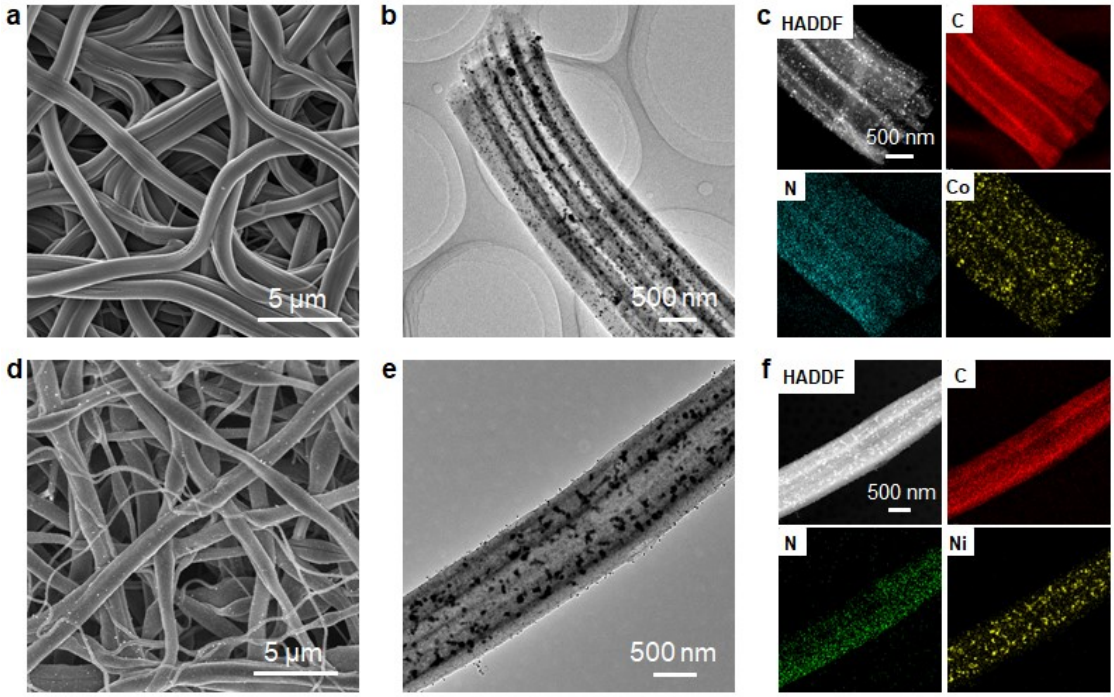


Fig. S6. a) SEM, b) TEM, and c) HAADF-STEM images and elemental mapping of Co/MNCFs-800. d) SEM, e) TEM, and f) HAADF-STEM images and elemental mapping of Ni/MNCFs-800.

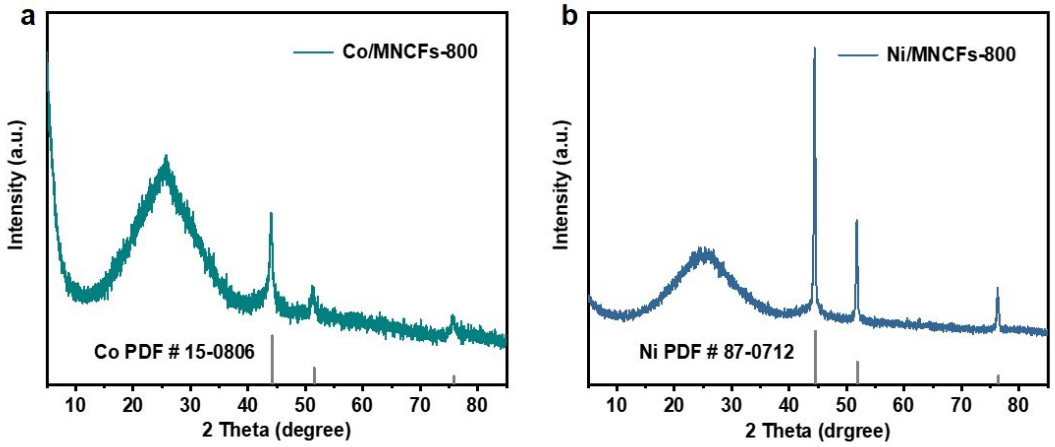


Fig. S7. XRD patterns of a) Co/MNCFs-800 and b) Ni/MNCFs-800.

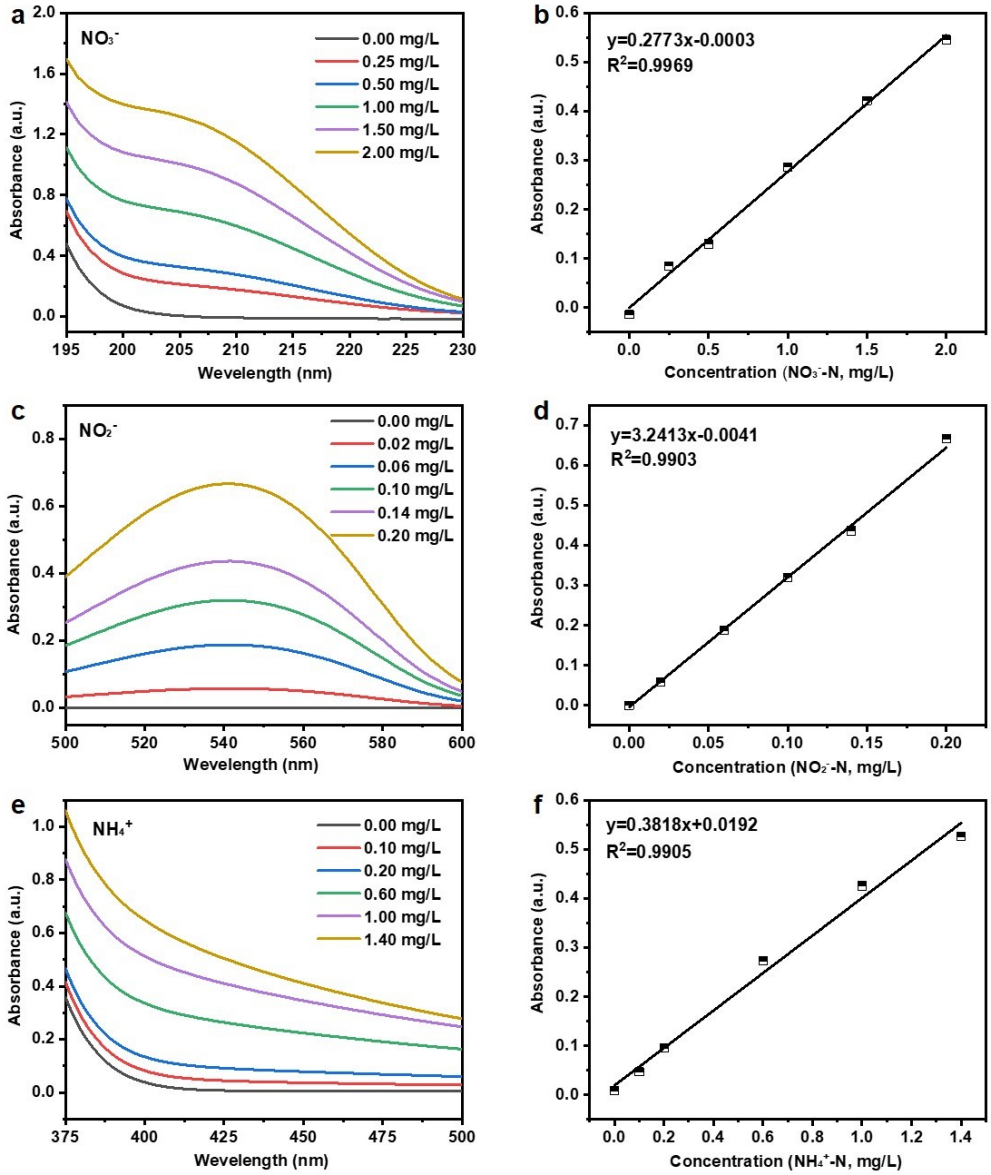


Fig. S8. The UV-vis absorbance spectra of a) $NO_3^-$-N, c) $NO_2^-$-N and e) $NH_4^+$-N, and their concentration-absorbance calibration curves of b) $NO_3^-$-N, d) $NO_2^-$-N, and f) $NH_4^+$-N. The calibration curves all showed good linearity.

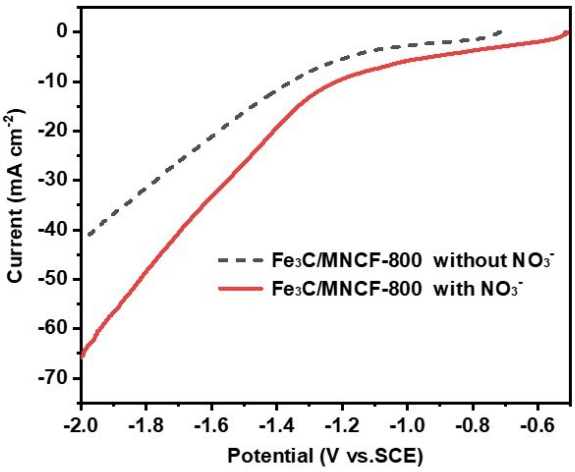


Fig. S9. LSV curves for the $Fe_3C$/MNCFs-800 in 0.1M $Na_2SO_4$ with and without 100 ppm $NaNO_3$ addition.

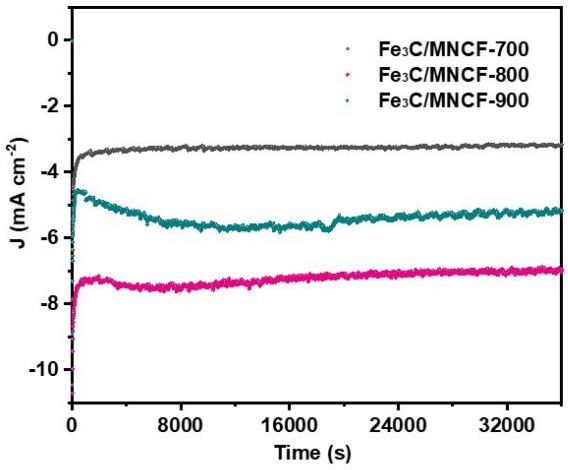


Fig. S10. The chronoamperometry curves of $Fe_3C$/MNCFs-x at -1.3 V vs. SCE.

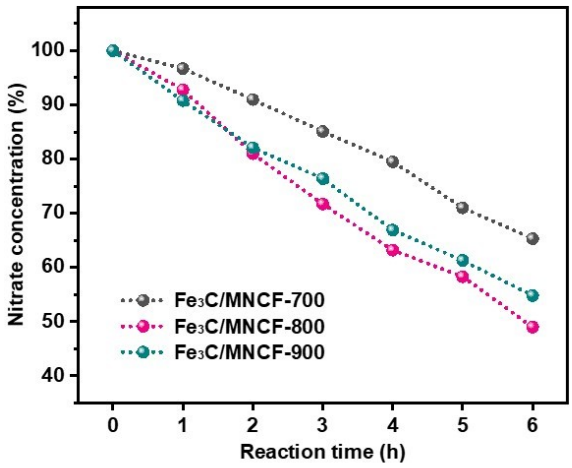


Fig. S11. The change of nitrate residual during the $NO_3RR$ process on $Fe_3C$/MNCFs-x.

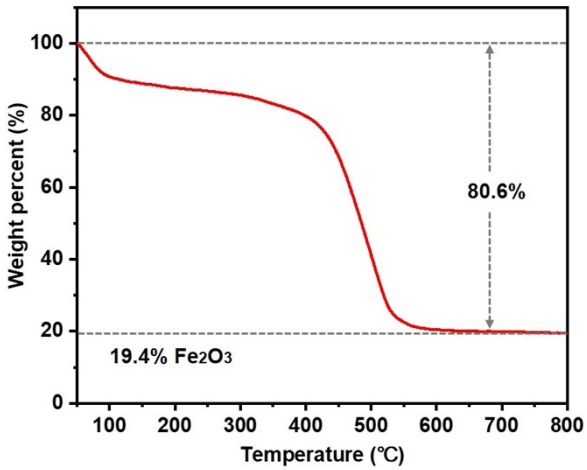


Fig. S12. TGA curves of $Fe_3C$/MNCFs-800.

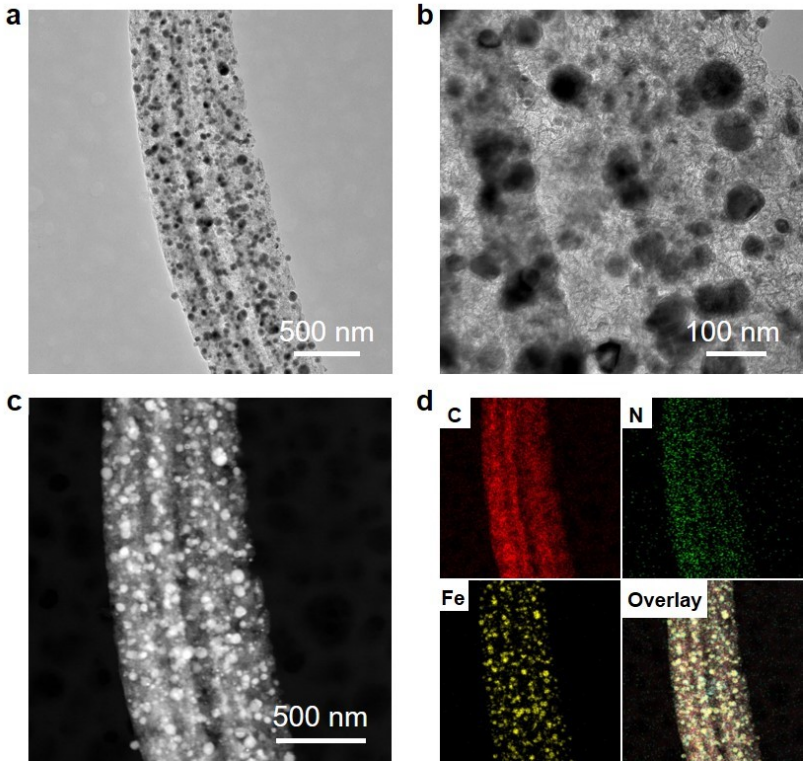


Fig. S13. a, b) TEM images, c) HAADF-STEM and d) corresponding elemental mapping images of $Fe_3C$/MNCFs-800 after 15 cycles (24 hours per cycle).

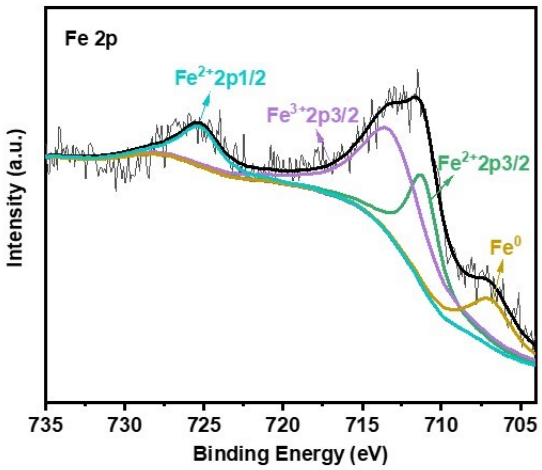


Fig. S14. Fe 2p of $Fe_3C$/MNCFs-800 after electrocatalytic nitrate reduction.

Table S1. Comparison of this work with previously reported Fe-based electrocatalysts.

| Materials | Electrolyte | Reaction time (h) | $NO_3^-$ Conversion (%) | $N_2$ selectivity (%) | Nitrate removal capacity (mg N/$g_{Fe}$) | Refs. |
|---|---|---|---|---|---|---|
| Fe@Gnc | 0.02M $Na_2SO_4$+0.02M NaCl | 24 | 72.7 | 99.6 | / | 34 |
| FeNi/g-mesoC/NF | 0.05 M $Na_2SO_4$+0.02 M NaCl, | 24 | 88 | 100 | 816 | 35 |
| Fe/$Fe_3C$-NCNF | 0.01M $Na_2SO_4$+0.03M NaCl | 24 | ~60 | 96 | 1787 | 36 |
| Fe/GF | 0.03M $Na_2SO_4$+0.01M NaCl | 24 | 67.7 | 96.6 | / | 37 |
| B-Fe NCs | 0.02M $Na_2SO_4$+0.02M NaCl | 24 | 80 | 99 | / | 38 |
| CL-Fe@C | 0.1M $Na_2SO_4$+0.02M NaCl | 24 | 42 | 98 | 1816 | 39 |
| RL-$Fe_2N$@NC | 0.02M $Na_2SO_4$+0.02M NaCl | 24 | 86 | 96 | / | 40 |
| $Fe_3C$/MNCFs | 0.1M $Na_2SO_4$+0.02M NaCl | 24 | 90.9 | 99.53 | 4031 | This work |